Charge Transfer through Terthiophene End-Capped Poly(arylene ethynylene)s

Alison M. Funston,[†] Eric E. Silverman,[‡] John R. Miller,*[,†] and Kirk S. Schanze*[,‡]

Chemistry Department, Brookhaven National Laboratory, Upton, New York 11973, and Department of Chemistry, University of Florida, PO Box 117200, Gainesville, Florida 32611-7200

Received: August 15, 2003; In Final Form: November 26, 2003

Two poly(arylene ethynylene)s (PAEs) that are end-capped with α-terthiophene (T_3) groups were prepared and structurally characterized by proton NMR, GPC, and optical spectroscopy. One of the polymers (T_3PPE_{13}) features a backbone structure that alternates phenylene ethynylene and bis(alkoxy)phenylene ethynylene repeat units. The second T_3 end-capped polymer (T_3PBpE_{12}) features an alternating structure with biphenylene ethynylene and bis(alkoxy)phenylene ethynylene repeats. The absorption spectra of the T_3 end-capped polymers are almost the same as those of the corresponding "parent polymers" (PPE_{164} and $PBpE_{21}$, respectively) that lack the T_3 end-groups. By contrast, whereas the fluorescence spectra of the parent polymers is dominated by a blue fluorescence with $\lambda_{max} = 425$ nm, the emission spectra of the end-capped polymers contains a significant contribution of a green fluorescence ($\lambda = 500-550$ nm). This signals that the singlet exciton is efficiently trapped by the T_3 end groups. Pulse radiolysis studies were carried out on all of the poly(arylene ethynylene)s in an effort to characterize the spectra and dynamics of the cation and anion radicals of the polymers. Pulse radiolytically generated solvent holes, and solvated electrons were transferred to the PAEs at nearly diffusion controlled rates. The absorption spectra of the anion radicals of the PAEs were similar and featured two strong absorption bands, one in the visible ($\lambda = 600$ nm) and the second in the near-IR ($\lambda = 1600-2000$ nm). The cation radicals of the T_3 end-capped polymers also feature two absorption bands, one in the visible and the second in the near-IR. However, the spectra of the cation radicals of the T_3 end-capped polymers show important differences. Specifically, the cation radical spectra of T_3BpE_{12} and $PBpE_{21}$ are identical, which reveals that the hole is not trapped by the T_3 end-cap in the biphenylene polymer. By contrast, the cation radical absorption spectra of T_3PPE_{13} ($\lambda_{max} = 640$ and 1350 nm) and PPE_{164} ($\lambda_{max} = 600$ and 1950 nm) are distinctly different. This difference suggests that the hole is localized on the T_3 end-group in T_3PPE_{13}. Bimolecular hole-transfer experiments using bithiophene (T_2, $E^{\circ}_{ox} = 1.21$ V), terthiophene (T_3, $E^{\circ}_{ox} = 0.91$ V), and quaterthiophene (T_4, $E^{\circ\circ}_{ox} = 0.76$ V) with PPE_{164} and $PBpE_{21}$ allowed the determination of the oxidation potentials for the PAEs. The values are PPE_{164}, $E^{\circ}_{ox} = 0.91$ V; $PBpE_{21}$, $E^{\circ}_{ox} = 0.85$ V (all potentials vs SCE). The lower oxidation potential of the biphenylene based PAE explains why the hole is not trapped by the T_3 end-groups in T_3BpE_{12}. The dynamics of intrachain hole transfer in T_3PPE_{13} are much faster than the rate of hole transfer from the solvent, and on the basis of this result, the lower limit for intrachain hole transfer is determined to be $k_{HT} \geq 1 \times 10^8$ s^{-1}.

Introduction

Conjugated polymers have been the focus of considerable research and development during the past several decades.[1,2] Interest in this field is motivated by the variety of possible applications that exist for conjugated polymers as the active materials in electronic, electrooptical, and optical devices.[2] One of the major factors which make conjugated polymers viable candidates for electronic and electrooptical device applications is that they feature good transport properties for neutral (excitons) and charged (polarons and bipolarons) carriers. To understand how to improve and tune the transport properties of conjugated polymers, many investigations have explored structure−property relationships for carrier transport.[3−7] By and large, most of these investigations have examined carrier properties in solid-state materials using electronic and optical techniques.

We have an interest in understanding exciton and charge transport properties of single-chain conjugated polymers.[8−10] This concept is important, for example, in the field of molecular and nanoscale electronic devices, where it is envisioned that single conjugated oligomer or polymer chains will function as exciton and/or charge carriers.[11,12] One approach to the investigation of carrier transport in single chain conjugated polymers is to carry out investigations on the materials dissolved in liquid solution, where interchain interactions are minimized.[13] Several techniques have been used to explore the dynamics and efficiency of exciton transport along single conjugated polymer chains. One technique involves the use of conjugated polymer chains featuring recognition elements that bind small molecule traps (quenchers) for excitons.[14,15] For example, cyclophane units have been used to bind viologen traps, polypyridine units have been used to bind metal ion traps,[16−18] and pendant ionic groups have been used to bind oppositely charged metal ion and molecular ion traps.[8,10,19−21] An alternative approach involves the use of copolymerization methods that randomly incorporate trap sites into the conjugated polymer backbone or append the

* To whom correspondence should be addressed. John R. Miller. Telephone: 631 344 4354. Fax: 631 344 5815. E-mail: jrmiller@bnl.gov. Kirk S. Schanze. Telephone: 352 392 9133. Fax: 352 392 2395. E-mail: kschanze@chem.ufl.edu.

[†] Brookhaven National Laboratory.

[‡] University of Florida.

10.1021/jp0364396 CCC: $27.50
Published on Web 01/08/2004

SCHEME 1

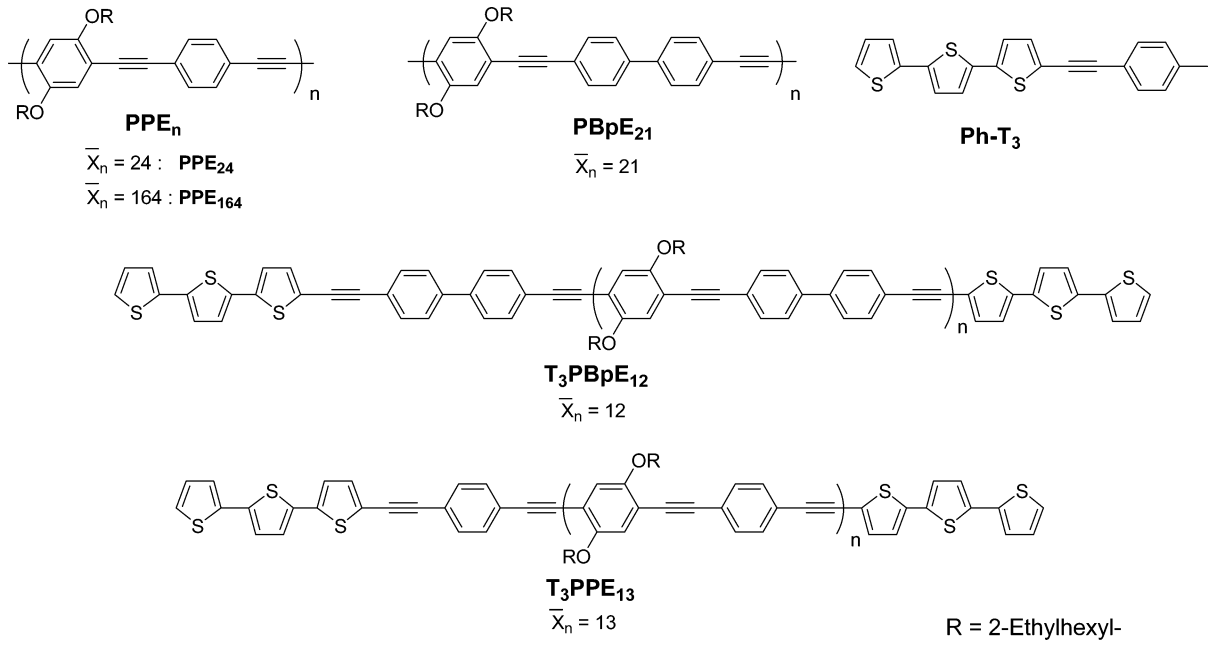

traps to the end of the conjugated polymer chains.[22−24] These studies have demonstrated that exciton transport along single conjugated polymer chains is both highly efficient and extraordinarily rapid.

Although a number of studies have examined exciton transport in single polymer chains in solution, only a few investigations have examined transport of charged carriers (e.g., radical cations).[13] To fill this void, we have initiated an investigation which seeks to use pulse radiolysis to investigate the spectroscopy and dynamics of radical cations and anions (polarons) in single conjugated polymer chains. The objective of our approach is to study conjugated polymers that feature end-caps designed so they will act as traps for cation (or anion) radicals on the main chain. Specifically, the necessary condition for a "trap" for radical cations is that the end-group have a lower oxidation potential relative to the potential for oxidation of the main chain, e.g., $E^{\circ}_{ox}(T) < E^{\circ}_{ox}$ (polymer), where T represents the hole trap moiety.

In the present manuscript, we report the results of an investigation of a series of poly(arylene ethynylene)s (PAE)s and poly(phenylene ethynylene)s (PPE)s that are end-capped with 2,2′:5′,2″-terthiophene (T_3) groups (Scheme 1). These polymers were designed to allow investigation of the spectroscopy and dynamics of cation radicals created on the single polymer chains by pulse radiolysis. PAE-type polymers were selected for this study for several reasons. First, PAEs are "rigid rod" polymers and as such are likely to adopt relatively extended conformations in solution. Consequently these materials represent models for extended, π-conjugated "molecular wires" of nanometer length. Second, this family of polymers can be synthesized relatively easily via Pd-mediated (Sonagashira) coupling methodology.[25] By varying the feed in the Sonagashira polymerization reaction, it is possible to end-cap the PAE chains and to control the degree of polymerization (i.e., the average chain length). The T_3 end groups were selected because it was anticipated that the necessary condition for hole-transfer from the PAE-chain to the T_3 end-groups would be satisfied, i.e., $E^{\circ}_{ox}(T_3) < E^{\circ}_{ox}$(PAE). In addition, because the spectroscopy of oligothiophene cation radicals has been investigated extensively, it was anticipated that it would be possible to distinguish the spectra of the PAE chain localized hole, $PAE^{+\bullet}$, from the end-group trapped hole state, $T_3^{+\bullet}$.

A long-term objective of this effort is to use ultrafast pulse radiolysis techniques[26] to measure the dynamics of radical ion diffusion along the backbone to the end-group trap sites, e.g., as illustrated for a cation radical

$$T_3\text{-(PAE)-}T_3 \xrightarrow{h^+} T_3\text{-(PAE}^{+\bullet}\text{)-}T_3 \xrightarrow{k_{HT}} T_3\text{-(PAE)-}T_3^{+\bullet} \quad (1)$$

where PAE represents the poly(arylene ethynylene), T_3 is a terthiophene end-group hole-trap, h^+ is a hole injected by pulse radiolysis, and k_{HT} is the (average) rate of transfer of the hole from the PAE chain to the T_3 trap. On the basis of the results presented herein, we are only able to provide a lower limit for k_{HT}; nevertheless, this study provides considerable insight into the structure, dynamics, and spectroscopy of PAE-based polarons. Indeed, to our knowledge, this is the first report concerning the thermodynamics and spectroscopy of polarons on PAE-type polymers.

Experimental Section

Materials and General Synthesis. 1,2-Dichloroethane (Aldrich) was HPLC grade and dried over 4 Å molecular sieves prior to use. Anhydrous 99.8% toluene (Aldrich) was used as received. Tetrahydrofuran (Aldrich, anhydrous) was distilled from $LiAlH_4$ and then from sodium/benzophenone and stored in an environment of argon. 2,2′-Bithiophene, 2,2′:5′,2″-terthiophene (T_3), 2,2′:5′,2″:5″,2‴-quaterthiophene (T_4), tetramethylphenylenediamine (TMPD), tetracyanoethylene (TCNE), 2,3,5,6-tetrachlorobenzoquinone (chloranil), 1,4-iodobenzene, 1,4-dimethoxybenzene, $Pd(PPh_3)_4$, and CuI were purchased from Aldrich or Acros. Quaterthiophene was recrystallized from toluene, and 2,2′-bithiophene, TMPD, TCNE, and chloranil were sublimed prior to use, and the other compounds were used as received. 2-Iodo-5:2′,5′:2″-terthiophene ($I-T_3$) was prepared by a literature procedure.[27] Chromatography was carried out using silica gel (Merk, 230−400 mesh). NMR spectra were obtained on Varian Gemini or VXR spectrophotometers operating at 300 MHZ or an Inova spectrophotometer operating at 500 MHZ.

Detail regarding the synthesis of all monomers is provided as Supporting Information.

Ph-T_3. To a Schlenk flask charged with THF (5 mL) and disopropylamine (DIPA, 3 mL) was added 2-iodo-α-terthienyl (20 mg, 0.154 mmol) and 1-ethynyl-4-methyl benzene (163 mg, 324 mmol). The resulting solution was degassed by 30 min of bubbling with argon. Copper (I) iodide (5 mg) and $Pd(PPh_3)_4$ (5 mg) were added while a positive pressure of argon was maintained, and the reaction mixture was heated to 60 °C. A voluminous precipitate formed within five minutes. After stirring overnight, and cooling to room temperature the mixture was diluted with 30 mL of ether and extracted with water (1 × 25 mL), $HCl_{(aq)}$ (1 N, 2 × 25 mL) and then brine (1 × 20 mL). The organic layer was dried over Na_2SO_4, and the solvent was removed by rotory evaporation. The resulting yellow oil was then dried under vacuum (0.1 mmHg) to remove excess 1-ethynyl-4-methyl benzene, affording the desired compound as an orange solid (45 mg, yield 98%). ^{1}H NMR ($CDCl_3$): δ 2.37 (s, 3 H), 7.03 (d, 1H), 7.05(dd, 1H), 7.06 (d, 1H), 7.15(d, 1H), 7.16 (m, 3H),7.18 (d, 1H) 7.23 (d, 1H), 7.41 (d, 2H). ^{13}C NMR ($CDCl_3$): δ 21.8, 82.2, 94.9, 120.0, 122.6, 123.7, 124.5, 124.6, 125.0, 128.1, 129.5, 131.5, 132.8, 135.7, 136.3, 138.4, HRMS: Calcd for $C_{21}H_{14}S_3$: 362.0257. Found: 362.0258.

PPE_{211}. To a solution of THF and DIPA (1:1, 1.5 mL) were added equimolar amounts of 2,5-bis-(2-ethylhexyloxy)-1,4-diiodobenzene (293 mg, 0.5 mmol) and 1,4-diethynylbenzene (63 mg, 0.5 mmol). The flask was fitted tightly with a rubber septum, and the solution was deoxygenated by applying a vacuum (from an aspirator) and argon consecutively over four iterations to the system using a syringe needle though the septum. Another solution of THF and DIPA (1:1, 1.5 mL) was prepared in an ampule and deoxygenated by the same method. To this solution was added $Pd(PPh_3)_4$ (17 mg, 0.017 mmol) and CuI (2 mg, 0.011 mmol). The resulting suspension was deoxygenated again, and sonication was applied to dissolve the catalysts. The monomer solution was added to the solution of catalyst (in the ampule) via syringe, the reaction solution was placed under vacuum, and the ampule was sealed. A voluminous precipitate, believed to be alkylammonium iodide, formed in less than five minutes. The solution was heated at 50 °C for 16 h with stirring in the dark. After this time, the seal was broken, and the solution was poured into methanol to precipitate the polymer, which was then filtered (but not allowed to dry completely) and redissolved in a small volume (<25 mL) of chloroform. The precipitation and redissolution process was repeated five times. Note that the polymer cannot be redissolved after it has been recovered as a dry solid film by evaporation from a solution of a good solvent (e.g., chloroform or toluene). Except as noted below the other PPE-based polymers behaved similarly. Thus, the material was stored as a stock solution in toluene that was kept in the dark. To obtain NMR spectra in a deuterated solvent it was necessary to recover the polymer from the nondeuterated solvent as follows. The chloroform solution of the polymer was diluted with a mixture of acetone and hexanes (both of which are poor solvents for the polymer) to afford a precipitate that was isolated by centrifugation and decanting. The resulting precipitate was then redissolved in the deuterated solvent for NMR analysis. Nevertheless, even using this procedure, it was not possible to obtain samples that were entirely free of nondeuterated solvent, and consequently some of the peaks in the NMR spectrum are partially obscured by peaks arising from the residual solvent (yield after precipitations, 250 mg, 55%). GPC (THF): M_n = 96 300, M_w = 183 000, PDI = 1.9. ^{1}H NMR ($CDCl_3$): δ 0.8−1.9 (m, obscured by solvent), 2.14 (m, 4.6 H), 2.15 (m, obscured by solvent), 3.8−3.9 (m, 13.6 H), 4.17 (t, 4 H), 7.0 (s, 1.89 H), 7.45 (s, 4.0 H).

A second batch of PPE was prepared under the same conditions. The NMR spectrum of this sample was identical to that listed above for PPE_{211}. The GPC of the second batch gave M_n = 74 800 and PDI = 2.1. This sample is referred to as PPE_{164} throughout the text.

PPE_{24}. This polymer was prepared by the same method as PPE_{211}, except that iodobenzene (12 mg, 0.06 mmol) was added to the monomer solution before degassing (isolated yield 242 mg, 53%). GPC (THF): M_n = 10 800, M_w = 32 400, PDI = 3.0. ^{1}H NMR ($CDCl_3$): δ 0.8−1.9 (m, integral obscured by solvent), 2.14 (m, 4.6 H), 2.15 (m, integral obscured by solvent), 3.8−3.9 (m, 13.6 H), 4.17 (t, 4H), 7.0 (s, 1.89 H), 7.45 (s, 4.0 H).

$PBpE_{21}$. This polymer was prepared and purified by the same method as PPE_{211}, except 4,4′-diethynylbiphenyl (100 mg, 0.5 mmol) was substituted for 1,4-diethynylbenzene, and the reaction was quenched after 10 h. $PBpE_{21}$ was readily soluble in THF and $CHCl_3$ even after being taken to dryness (isolated yield 254 mg, 48%). GPC (THF): M_n = 11 300, M_w = 18 100, PDI = 1.6. ^{1}H NMR ($CDCl_3$): δ 0.8−1.8 (broad m, 43 H), 3.5 (s, 0.39 H), 3.86 (b, 4.3 H), 7.05 (s, 1.81 H), 7.2, (s, 8 H).

T_3PPE_{13}. This polymer was prepared by the same method as PPE_{211}, except that 2-iodo-α-terthienyl (19 mg, 0.05 mmol) was added to the monomer solution before degassing (isolated yield 261 mg, 57%). GPC (THF): M_n = 6450, M_w = 13 600, PDI = 2.1. ^{1}H NMR ($CDCl_3$): δ 0.8−1.9 (m, integration obscured by solvent) 3.9 (m, 5 H),2 6.9 (d, 0.23 H), 7.0 (s, 1.55 H), 7.4 (s, 4.0 H). IR(thin film): cm^{-1} 2958 (s), 2926(s), 2862 (m), 1596 (w), 1516 (m), 1489 (m), 1463 (m), 1415(m), 1383 (m), 1276 (m), 1212 (s), 1117 (w), 1031 (m), 835 (m), 718 (w).

T_3PBpE_{12}. This polymer was prepared and purified by the same method as PPE_{211}, except 4,4′-diethynylbiphenyl (100 mg, 0.5 mmol) was substituted for 1,4-diethynylbenzene and an additional compound, 2-iodo-α-terthienyl (19 mg, 0.05 mmol), was added to the solution of monomers before degassing, and the reaction was allowed to run for 16 h. T_3PBpE_{12} was readily soluble in THF and $CHCl_3$ even after being taken to dryness (isolated yield 230 mg, 43%). GPC (THF); M_n = 7200, M_w = 18 100, PDI = 2.5. ^{1}H NMR ($CDCl_3$): δ 0.8−1.8 (br, m, 30 H), 3.86, (b, 4 H), 6.6 (b, 0.22 H), 6.8, (s, 0.32 H) 7.05 (s 1.5 H), 7.6 (s, 8H). IR (thin film): cm^{-1} 2958 (s), 2915 (s), 2872 (s), 1644 (w) 1606 (w), 1505 (m), 1462 (m), 1415 (m), 1272 (w), 1206 (m), 1120 (w), 1031 (m), 999 (w), 855 (w), 820 (m).

Photophysical Methods. UV−visible absorption spectra were obtained on a Varian Cary 100 spectrophotometer. Corrected steady-state emission spectra were recorded on a SPEX F-112 fluorescence spectrophotometer. Samples were contained in 1 cm × 1 cm quartz cuvettes, and the optical density was adjusted to approximately 0.1 at the excitation wavelength. Emission quantum yields are reported relative to perylene (Φ_{em} = 0.94),[28] and an appropriate correction was applied for the difference in refractive indices in the sample and actinometer solvent.[29] Time-resolved emission decays were obtained by time-correlated single photon counting on an instrument that was constructed in-house. Excitation was effected by using a violet diode laser (IBH instruments, Edinburgh, 405 nm, pulse width 800 ps). The time-resolved emission was collected using a red-sensitive, photon counting PMT (Hamamatsu, R928), and the light was filtered using 10 nm band-pass interference filters. Lifetimes were determined from the observed decays with the DAS6 deconvolution software (IBH Instruments, Edinburgh, Scotland).

GPC was preformed using a Rainin Dynamax model SD-200 solvent delivery system equipped with two PL-Gel 5 micron Mixed D columns (Polymer Laboratories, Inc., Amherst, MA) connected in series and a UV detector set at a wavelength where the polymer absorbs. Molecular weight information was calculated from the chromatograms using Polymer Laboratories software.

Radiation Techniques. This work was carried out at the Brookhaven National Laboratory Laser-Electron Accelerator Facility (LEAF). The facility has been described elsewhere.[26,30] The electron pulse (≤120 ps duration) was focused into a quartz cell with an optical path length of 20 mm containing the solution of interest. For the polymer solutions, the concentration of repeat units used was typically 0.2−2 mM. The monitoring light source was a 75 W Osram xenon arc lamp pulsed to a few hundred times its normal intensity. Wavelengths were selected using either 40 or 10 nm band-pass interference filters. Transient absorption signals were detected with either FND-100Q silicon (≤1000 nm) or GAP-500L InGaAs (≥1100 nm) diodes and digitized with a Tektronix TDS-680B oscilloscope. The transmission/time data were analyzed with Igor Pro software (Wavemetrics). Reaction rate constants were determined using a nonlinear least-squares fitting procedure described previously. This procedure accounts for geminate recombination, which is encountered on the time scales investigated. Bimolecular rate constants were determined using the linearity of the observed pseudo-first-order growth of the product with respect to the solute concentration. Where not stated, uncertainties are 15%. Bimolecular reactions of PAE ions with charge acceptors often went to completion with no detectable $PAE^{+\bullet}$ remaining. However, in others including most reactions with terthiophene, the kinetics proceeded to equilibria in which substantial fractions of the $PAE^{+\bullet}$ remained from which equilibrium constants could be calculated. Molar extinction coefficients of the radical cations were calculated using $G(DCE^{+\bullet}) = 0.68$,[31] where G is the radiation chemical yield (molecules produced/100 eV). For the anions, the reported G values for the electron in THF has varied greatly. The value used was $G(e^-_{THF}) = 0.53$, the average of a number of reported values.[32]

The total dose per pulse was determined before each series of experiments by measuring the change in absorbance of the electron in water. The dose received was calculated using $\epsilon(700\text{ nm}, e^-_{aq}) = 18\,830\ M^{-1}\ cm^{-1}$ and $G(e^-_{aq}) = 2.97$. The dose was corrected for the difference in electron density of the organic solvents used compared to that of water. Radiolytic doses of 5−18 Gy were employed. For the DCE/toluene solutions, dissolved oxygen was removed by purging with argon gas for at least 10 min, and the cells were then sealed with septa and Parafilm. Solutions in THF were prepared in an argon environment and sealed under argon with Teflon vacuum stoppers. Samples were prepared immediately prior to use. During irradiation, samples were exposed to as little UV light as possible to avoid photodecomposition, although no evidence of this occurring was found within the time frames monitored. Measurements were carried out at 21 °C.

Results and Discussion

Polymer Synthesis and Structural Characterization. The chemical structures and acronyms for the PAEs that are the focus of this work are shown in Scheme 1. The numerical subscript in the acronyms indicates the number average degree of polymerization, $\bar{X}_n$, as calculated from the GPC-derived M_n values and the molecular weight of the polymer repeat units. For end-capped polymers, $\bar{X}_n$ represents the number of arylene ethynylene repeats, and does *not* include end-groups. Note that in the PPE and PBpE chains each repeat unit contains two phenylene and three phenylene rings, respectively.

All of the polymers synthesized in the course of this work were prepared in AA + BB type polymerization reactions using Sonagashira coupling methodology.[14,15,22,37] The "parent polymers", PPE_{164} and $PBpE_{21}$, were prepared using equimolar amounts of the monomers, whereas the terthienyl (T_3) end-capped polymers were prepared as shown in eq 2 below. For the end-capped polymers, it was found that the use of a stoichiometric excess of the aryl iodide functional group gave moderate M_n values. In addition, a poly(phenylene ethynylene) with $\bar{X}_n = 24$ and thus a molecular weight comparable to that of the end-capped polymer, was synthesized according to eq 2 with iodobenzene used in place of iodoterthiophene (I−T_3).

The end-group "model" Ph-T_3 was synthesized via condensation of *p*-ethynyltoluene and I−T_3. The Ph-T_3 model compound was designed to mimic the polymer end-groups which feature T_3 adjacent to phenylene units in T_3PPE_{13}.

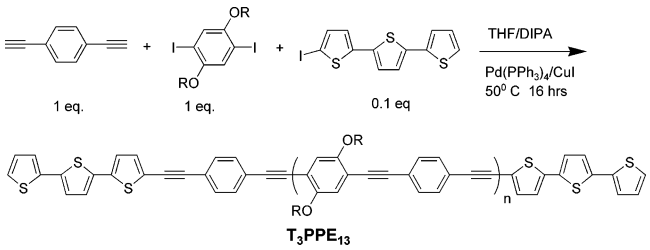

T_3PPE_{13}

Each of the polymer samples was analyzed by gel permeation chromatography (polystyrene standards) and by proton NMR spectroscopy. The ^1H NMR spectra of the end-capped polymers exhibit resonances in the aromatic region (δ = 6.5−7.5 ppm) that are not observed in the spectra of the parent polymers. On the basis of comparison of spectra of the end-capped polymers with that of the T_3−Ph model compound, it is believed that these resonances arise from the T_3 end-groups, confirming their existence in the polymers. To use NMR peak integration to estimate $\bar{X}_n$ for the polymers, we take advantage of the fact that in the end-capped polymers the ratio of phenylene (or biphenylene) to dialkoxyphenylene units is $(n + 1):n$, where n is the chain length (refer to structural diagrams in Scheme 1). Thus, by measuring the ratio of the integral values for the dialkoxybenzene and phenylene (or biphenylene) repeats, it is possible to estimate $\bar{X}_n$. This NMR integration-based approach yielded values of $\bar{X}_n = 7$ and 8 for T_3PPE_{13} and T_3PBpE_{12}, respectively.[38] Note that $\bar{X}_n$values determined by NMR integration are less than those established by GPC. This finding is consistent with previous work that shows that GPC tends to overestimate $\bar{X}_n$ in rigid-rod conjugated polymers such as the PPEs that are the focus of the present investigation.[39−42] Nonetheless, GPC remains the most commonly used method to obtain information about the molecular weight of conjugated polymers.

Absorption and Fluorescence Spectroscopy. Absorption and fluorescence spectra were obtained on dilute samples of the polymers ([PRU] = 2 μM, where PRU is polymer repeat units) in THF solution. Similar results were obtained on the phenylene and biphenylene based systems; therefore, for brevity, we discuss only the results for the phenylene series. Figure 1 shows the absorption and fluorescence of PPE_{164}, T_3PPE_{13}, T_3, and the end-group model Ph-T_3. The spectra of PPE_{24} are not included, as they were identical to those of the higher molecular weight sample, PPE_{164}. The molar absorptivity values of the

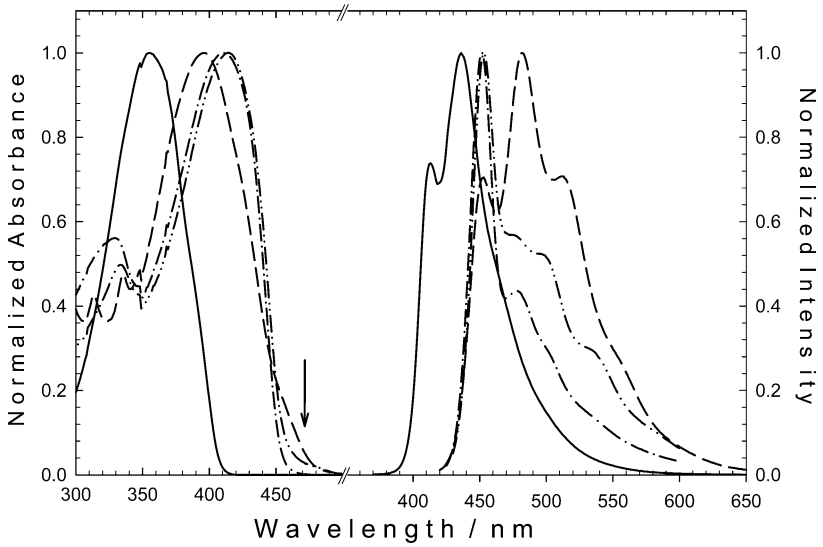

Figure 1. Absorption (left) and photoluminescence (right) spectra of poly(phenylene ethynylene)s and end group model compounds. (—): T_3; (– – –): Ph-T_3; (—•—•): PPE_{164}; (—••—••): T_3PPE_{13}.

parent and end-capped polymers along with selected fluorescence lifetime data are provided as Supporting Information.

The absorption and fluorescence spectra of PPE_{164} are very similar to the spectra of structurally similar PPEs.[37,43] In particular, the absorption spectrum is dominated by an intense band which is due to the allowed, long-axis polarized π,π^* transition, while the fluorescence appears as a relatively narrow band that is dominated by the zero phonon transition. The small Stokes shift and weak vibronic structure present in the fluorescence indicate that there is relatively weak electron-vibrational coupling in the relaxed singlet excited state. The absorption spectrum of T_3 end-capped polymer T_3PPE_{13} is nearly identical to that of the PPE_{164} parent, except for a weak "tail" on the low energy side of the band (see arrow in Figure 1). The fact that the absorption spectra of PPE_{164} and T_3PPE_{13} are similar is not surprising, given that the T_3 end groups are present at a relatively low concentration relative to the PPE backbone. The "tail" on the absorption band of T_3PPE_{13} is likely due to the T_3 end groups.

The difference in the fluorescence of the parent and end-capped polymers is readily apparent by eye: under near-UV illumination, the fluorescence of PPE_{164} is blue, whereas that of T_3PPE_{13} has a distinct green hue. At first glance, the data suggest that the emission from T_3PPE_{13} arises primarily from the PPE backbone, with a contribution from a state that is localized on the T_3 end groups. However, comparison of the fluorescence data for the polymers with that of T_3 and the end-group model Ph-T_3 suggests a more complicated situation. As shown in Figure 1, the absorption and fluorescence spectra of T_3 are blue-shifted considerably from the corresponding spectra of both PPE_{164} and T_3PPE_{13}. This clearly indicates that an excited state which is "localized" on T_3 is at a higher energy than the PPE $^1\pi,\pi^*$ exciton. However, the absorption and fluorescence spectra of end-group model Ph-T_3 are red-shifted considerably from those of T_3. Furthermore, there is a similarity, both in energy and vibronic structure, between the fluorescence spectra of Ph-T_3 and T_3PPE_{13}.

The fact that the absorption and fluorescence spectra of Ph-T_3 are red-shifted considerably relative to that of T_3 indicates that there is substantial delocalization of the ground and excited-state wave functions of T_3 into the phenylene ethynylene substituent. Indeed, molecular orbital calculations carried out on a T_3 end-capped model oligomer (outlined below) clearly reveal that, although both the HOMO and LUMO have significant population on the T_3 units, they are also substantially delocalized into the PPE. Thus, we conclude that in T_3PPE_{13} the singlet excited-state derives from a configuration interaction of states localized on the T_3 end-cap and with states on the PPE backbone. The fact that the fluorescent excited state is a composite of PPE and T_3 character is supported by the fact that the fluorescence spectrum is essentially independent of the excitation wavelength, even for excitation into the tail of the absorption band, where the absorption is believed to be dominated by the T_3 end-groups.

Fluorescence lifetime measurements also support the concept of excited-state delocalization in T_3PPE_{13} (the table in the Supporting Information). Specifically, the fluorescence decay characteristics of T_3PPE_{13} are very similar to those of PPE_{164}. For both polymers, the decay kinetics are dominated by a short lifetime component ($\tau \approx 0.5$ ns), even when the fluorescence is monitored at 550 nm, which corresponds to the "green" emission from the T_3 end-groups. The short fluorescence lifetimes characteristic of conjugated polymers are due, in part, to very high radiative decay rates, which in turn arise due to the extended π-conjugation. The fact that the fluorescence decay of T_3PPE_{13} is fast and relatively wavelength independent supports the premise that the emitting state is strongly delocalized and has mixed T_3 and PPE character. If this were not the case, we would expect that the emission decays would be wavelength dependent, and in the longer wavelength region (where the emission is dominated by the T_3 groups) the lifetime would be considerably longer.

The fluorescence results obtained on T_3PPE_{13} are also interesting when compared to data reported by Swager, Gil, and Wrighton on a PPE polymer that is end-capped with anthracene groups linked through the 9-position.[22] In the 9-anthracenyl end-capped polymer, the fluorescence of the PPE chain is almost entirely quenched and it is replaced by a red-shifted fluorescence that is assigned to the 9-anthracenyl end-groups. The surprising feature is that the PPE-based fluorescence is quenched in the 9-anthracenyl system, even though the difference in energy between the PPE- and 9-anthracenyl-based excited states is similar to the difference in the energies of the PPE- and T_3-based excited states. It is possible that the difference in the two end-capped systems lies in the difference in molecular orbital and excited-state symmetries of the end-capping groups. Thus,

in the T_3 end-capped system, the T_3-localized molecular orbitals and states are of the same symmetry as those on the PPE backbone, allowing strong excited-state mixing to occur. However, by contrast, in the 9-anthracenyl- end-cap system, the lowest excited-state localized on the 9-anthracenyl unit is polarized perpendicular to the PPE-chain. As a result, mixing between the PPE-based excitation and states localized on the 9-anthracenyl chromophore is low, resulting in a "trap" state that is localized on the end-group.

Radiolytic Production of Radical Cations and Anions. Pulse radiolysis was used to produce the ion radicals on the parent and end-capped PAEs in solution. The process of generating the PAE-based ion radicals involves a series of preceding reactions in which the high energy electron pulses are converted to strongly oxidizing solvent holes (h^+) or solvated electrons (e_s^-) which then are transferred to the PAE chains. Therefore, prior to discussing the details concerning the dynamics and spectroscopy of the PAE ion radicals, we provide an overview of the relevant aspects of the radiation chemistry techniques used.

The pulse radiolysis technique utilizes short pulses of electrons, and at the LEAF facility, these electrons have an energy of 10 MeV and the pulse width is <120 ps. Although the primary electrons pass completely through the solution and exit the spectrophotometric cell, each primary electron produces $\sim 10^4$ ionizations in the solution that result in a few μM of thermalized solvated electrons (e_s^-), and a corresponding number of radical cations of solvent molecules. In 1,2-dichloroethane (DCE), the electrons are immediately captured by solvent molecules to form radicals and Cl^- ions;[31,45] in tetrahydrofuran (THF), the solvent cation radicals decompose to radicals and solvated protons. The net effect of the electron pulses is therefore to produce thermalized solvent cation radicals (h^+) in DCE and thermalized solvated electrons (e_s^-) in THF. Because the holes in DCE and electrons in THF must diffuse to attach to the conjugated polymers or other solutes such as thiophene oligomers, the desired ions of the molecules are formed in bimolecular processes. Because the PAEs (or thiophene oligomers) are present in excess, these bimolecular reactions are pseudo first-order, and the observed h^+ and e_s^- transfer rates to the PAEs depend on polymer concentration and the bimolecular rate constant for reaction of h^+ or e_s^- with the polymer. Note that a fraction of the h^+ in DCE (and e_s^- in THF) is also lost due to reaction with counterions (Cl^- in DCE, protons and radicals in THF); however, these reactions are measured and accounted for in the measurements.

Because PPE_{164} and T_3PPE_{13} are not very soluble in pure DCE, experiments were carried out in "DCE/toluene", 1,2-dichloroethane with 1.6 M toluene (PhMe) added to solubilize the polymer. In the DCE/toluene solvent mixture, the hole which transfers charge to the polymer is $(PhMe)_2^{\bullet+}$ which is formed by rapid positive charge transfer from the solvent holes to toluene, followed by rapid dimer formation. The $(PhMe)_2^{\bullet+}$ ion, which absorbs near 1000 nm,[46,47] attaches to the PAEs with rate constants similar to those of DCE-based solvent holes. An additional oxidant, identified as a $Cl^{\bullet}-$toluene π-charge transfer complex, is produced in the DCE/toluene solutions. This complex slowly oxidizes species with E°_{ox} lower than 1.1 V (vs SCE) to produce the corresponding radical cation. The slow reaction rate of the complex with solutes along with the slow reaction rate of the polymers (see discussion below) results in little contribution to the polymer radical cation yield from this species, but it reacts more efficiently with some small molecules including terthiophene, leading to decreased certainty in the determination of equilibrium constants (see below). The radiation chemistry of the DCE/toluene solution is described in detail elsewhere.[48]

Electron and Hole Transfer to PAEs Following Radiolysis. A series of experiments were carried out in which the bimolecular rate constants for the h^+ and e_s^- trapping reactions were determined, i.e., k_{3a} and k_{3b}

$$\mathrm{PAE} + (\mathrm{PhMe})_2^{\bullet+} \xrightarrow[\mathrm{DCE/PhMe}]{} \mathrm{PAE}^{+\bullet} + 2\mathrm{PhMe} \quad (3a)$$

$$\mathrm{PAE} + e^-_s \xrightarrow[\mathrm{THF}]{} \mathrm{PAE}^{\bullet-} \quad (3b)$$

Reactions 3a and 3b are strongly exoergic ($\Delta G^\circ < -0.5$ eV) and occur with diffusion-controlled rates. Thus, before presenting and discussing the kinetic data, it is appropriate to consider the theory of diffusion of a small ion (a point charge) to a rigid-rod polymer such as the PAEs.

In recent years, theory has provided solutions to the problem of a mobile point diffusing to a number of spherical monomer units joined together in one, two, or three-dimensional arrays.[49,50] Traytak's [49,50] solution for one dimension and its recent test by Grozema[51] makes use of an effective reaction radius, R_{eff}, defined in terms of the reaction radius, R_{m}, for one unit (a monomer) and the number of units in the chain, n, as in eq 4

$$R_{\mathrm{eff}} = \frac{nR_{\mathrm{m}}}{1 + \dfrac{R_{\mathrm{m}}}{a}\ln(n)} \quad (4)$$

The diffusion-controlled rate of reaction with the chain of length n is then given by eq 5, which is identical in form to the classic solution of Smoluchowski[52] for reaction of spherical particles, where D is the sum of the diffusion coefficients of the reactants

$$k(t) = 4\pi R_{\mathrm{eff}} D(1 + R_{\mathrm{eff}}/(\pi D t)^{1/2}) \quad (5)$$

The second term in eq 5, often called the 'transient" term, contributes less than 10% at times longer than $10R^2/\pi D$. For small species with high diffusivity this time is generally less than a few nanoseconds, but Grozema demonstrated[51] that the large size of a polymer strand leads to a much larger effective reaction radius and a much larger and longer lived transient term. Although the steady-state, diffusion-controlled rate constant per repeat unit falls rapidly with the number of repeats, n, some of that loss is recovered due to the larger transient terms.[49,50] Although the "rate constant" is not in fact constant, it does not vary significantly during the time course of the h^+ and e_s^- transfer reactions. Thus, the experimentally observed pseudo-first order decays are very nearly exponential. Consequently, here we report effective or "average" rate constants, which represent best fits to the observed pseudo first-order kinetic traces for the rise of the absorption due to the PAE radical ions. Note that the rate constants would have somewhat different values if the range of polymer concentrations used were significantly higher or lower.

The effective rate constants for the bimolecular reactions of h^+ (in DCE/toluene) and e_s^- (in THF) formed via pulse radiolysis with the PAEs to produce the radical cations and anions (respectively) of the polymers are presented in Table 1. The bimolecular rate constants are reported both with respect to polymer and repeat unit concentration. Several points are of note with respect to the rate data. First, the experimentally determined rate constants for growth of the PAE radical ions when expressed per monomer repeat unit are significantly lower

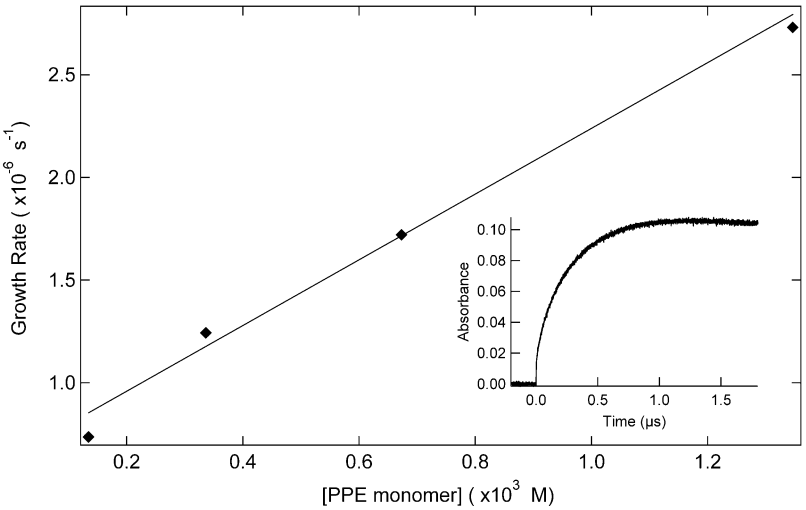

Figure 2. Observed rate of growth of PPE_{164} radical cation in DCE/toluene (1,2-dichloroethane + 1.6 M toluene) solution as a function of concentration in repeat units (the concentration of PPE molecules is smaller by a factor of 164). The straight line best fit yields a slope of 1.6×10^9 M^{-1} s^{-1} per repeat unit or 1.0×10^{11} M^{-1} s^{-1} using concentration of PPE chains. The inset is the observed growth of the PPE_{164} radical cation at 600 nm.

TABLE 1: Reaction Rate Constants of Poly(arylene ethynylene)s (PAEs) and Terthiophene End-capped PAEs with Positive and Negative Charge Carriers in Solution

polymer	n	k (M^{-1} s^{-1})	$k_{(monomer)}$ (M^{-1} s^{-1})[a]
$PPE_{164} + (Me\Phi)_2^{\bullet+}$	164	2.1×10^{11}	1.3×10^9
$PPE_{24} + (Me\Phi)_2^{\bullet+}$	24	4.8×10^{10}	2.0×10^9
$PBpE_{21} + (Me\Phi)_2^{\bullet+}$	21	5.1×10^{10}	2.4×10^9
$T_3PPE_{13} + (Me\Phi)_2^{\bullet+}$	13	7.1×10^{10}	5.5×10^9
$T_3PBpE_{12} + (Me\Phi)_2^{\bullet+}$	12	3.0×10^{10}	2.4×10^9
$T_2 + (Me\Phi)_2^{\bullet+}$		1.1×10^{10}	5.3×10^9
$T_3 + (Me\Phi)_2^{\bullet+}$		1.7×10^{10}	5.5×10^9
$T_3 + [Me\Phi{:}Cl^{\bullet}]$		5.0×10^9	1.7×10^9
$T_4 + (Me\Phi)_2^{\bullet+}$		*b*	*b*
$T_4 + [Me\Phi{:}Cl^{\bullet}]$		4.1×10^9	1.0×10^9
$PPE_{164} + e^-_{THF}$	164	4.7×10^{12}	2.8×10^{10}
$PBpE_{21} + e^-_{THF}$	21	1.3×10^{12}	6.3×10^{10}
$T_3PPE_{13} + e^-_{THF}$	13	7.1×10^{11}	5.5×10^{10}
$T_3PBpE_{12} + e^-_{THF}$	12	3.5×10^{11}	2.8×10^{10}

[a] For comparison to small molecules, the average rate constant per repeat unit is reported. For T_3-containing polymers, the T_3 was not included. [b] Could not be measured due to absorption of the product cation at 1000 nm.

than expected for a diffusion controlled reaction between two small molecule reactants. Second, in general, the rates for electron transfer to the PAEs (eq 3b) are considerably faster compared to those for hole transfer (eq 3a). This difference reflects the considerably larger diffusion rate of e_s^-.[53−56]

Poly(arylene ethynylene)s are known to aggregate in solution with the degree of aggregation being dependent upon the solvent system used and the concentration of the polymer.[20,57] The pseudo-first-order growth of $PPE_{164}^{\bullet+}$ as a function of polymer concentration, shown in Figure 2, is linear to a concentration of 1.35×10^{-3} M in repeat units, suggesting that aggregation is not significant in the DCE/toluene solutions at these concentrations, which were typical of the concentrations used in the paper. Because THF is a better solvent for the polymers than the DCE/toluene solvent mixture, aggregation is not likely in that medium.

The species having the spectrum attributed to $PPE_{164}^{\bullet+}$ reacts with TMPD, a good hole scavenger, with a bimolecular rate $k = 2.8 \times 10^9$ M^{-1} s^{-1} to produce $TMPD^{\bullet+}$ with well-known absorbance bands at 570 nm and 620−630 nm.[58] Similarly $PPE_{164}^{\bullet-}$ produced in THF reacts with tetracyanoethylene (TCNE) and 2,3,5,6-tetrachlorobenzoquinone (chloranil) as

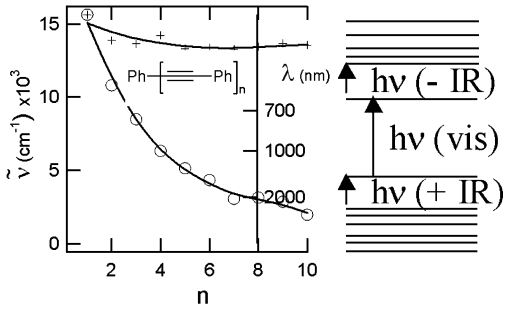

Figure 3. Transition energies computed for radical cations of phenylene ethynylene oligomers as a function of length, n. The energy of the lowest allowed transition (○) is very sensitive to length, while the energy of the strong transition in the visible (+) changes little with *n*. The simple MO diagram at right indicates the nature of the transitions, determined from the CI calculation. Calculations were ZINDO/S for AM1u geometries of the cations.

electron acceptors with rates in the range $1-2 \times 10^{10}$ M^{-1} s^{-1} to produce species with peaks at 450 nm, characteristic of the corresponding radical anions.[58] On the basis of these hole and electron-transfer experiments, we conclude that PAE-based radical cations ($PAE^{\bullet+}$) are the predominant species formed in DCE/toluene solution and PAE-based radical anions ($PAE^{\bullet-}$) are produced in THF.

Semiempirical Calculations: Spectroscopy of PPE-Based Ion Radicals. Prior to discussing the experimentally determined spectra of the PAE-based ion radicals, it is helpful to use theory to provide insight into the nature of the expected electronic transitions. Thus, semiempirical calculations (ZINDO/S, CI = 6,6, AM1u geometries) on a series of PPE-type model oligomers, $[Ph-(-C\equiv C-Ph-)_n-H]^{\bullet+}$ (structure in Figure 3), were carried out.[59] The Zindo/S calculations predict two optical transitions with energies that decrease with increasing oligomer length, *n* (Figure 3). Except for the shortest member of the series (i.e., diphenylacetylene, $n = 1$), the lowest energy transitions in the radical cations derive primarily from a strongly allowed, one-electron transition from the HOMO − 1 to the half-occupied HOMO (SOMO) as indicated schematically in Figure 3. (Here by HOMO and LUMO we refer to orbitals that are the highest occupied and lowest unoccupied in the neutral parent molecule.) The low-energy transition is predicted to occur in the near-IR region, and its energy is expected to vary strongly with the

length of the PPE segment. The calculations predict that the second, higher energy transition will occur in the visible region, and it consists primarily of HOMO (SOMO) → LUMO character. The calculations further predict that the energy of this transition varies only weakly with oligomer length. Calculations on the anion radicals give qualitatively similar results to those for the cation radicals; however, in this case, the near-IR bands derive primarily from the LUMO (SOMO) → LUMO + 1 transition (see Figure 3).

Visible/Near-IR Spectroscopy of PAE Radical Cations and Anions. By monitoring the wavelength dependence of the transient absorption of PAE solutions at a fixed delay time following the e^- pulse, it is possible to construct the visible-near-IR absorption spectra of the PAE-based radical ions. The delay time used is dependent upon the concentration of polymer and the bimolecular rate constant for charge transfer from the solvent to the polymer. Generally in these experiments, the delay times used were of the order of 0.1−1.0 μs, following the growth of the radical ion species and prior to its decay. Based on radiolysis yields of $(PhMe)_2^{\bullet+}$ in DCE/toluene and e_s^- in THF, it is possible to estimate the molar absorptivity (ϵ, M^{-1} cm^{-1}) of the PAE radical ions. The resulting spectra for a variety of PAE-based radical ions are illustrated in Figure 4 along with spectra of the T_3 oligomer based radical ions.

First, we consider the spectra of the radical anions. Figure 4a compares spectra of $T_3^{\bullet-}$ and the biphenyl-based PAEs, $PBpE_{21}^{\bullet-}$ and $T_3PBpE_{12}^{\bullet-}$. All three anion radicals feature two absorption bands: one in the visible and a second, broad band in the near-IR. The two bands are intense (ϵ > 50 000 M^{-1} cm^{-1}). The observed spectra are qualitatively consistent with those predicted by the Zindo/S calculations, supporting their assignment to the PBpE-based anion radicals. The experimentally observed absorption bands occur at λ_{max} = 600 and 1100 nm in $T_3^{\bullet-}$, whereas in $PBpE_{21}^{\bullet-}$ and $T_3PBpE_{12}^{\bullet-}$, λ_{max} = 625 and >1600 nm. The most significant feature is that the spectra of $PBpE_{21}^{\bullet-}$ and $T_3PBpE_{12}^{\bullet-}$ are essentially identical, showing that the T_3 end-caps have no influence on the spectrum of $T_3PBpE_{12}^{\bullet-}$. This finding implies that the electron is not localized on the T_3 end-groups in the end-capped polymer; rather it is localized on the PBpE chain. This is consistent with expectation, given that T_3 is more electron rich than the PBpE chain, and therefore, the LUMO is likely at a lower level on the PBpE units. Another noteworthy feature is that the low energy band in the PBpE anion radicals is at considerably longer wavelength and is much broader than the analogous feature for $T_3^{\bullet-}$. This is consistent with the notion that the polaron is considerably more delocalized in the PBpE polymers than in $T_3^{\bullet-}$ where the charge is restricted to delocalization over only three thienyl rings.

Figure 4b compares the spectra of $T_3^{\bullet-}$ with the anion radicals of the phenylene-based polymers $PPE_{164}^{\bullet-}$ and $T_3PPE_{13}^{\bullet-}$. The spectra of the PPE-based anion radicals are very similar to those of the PBpE based systems, with two bands at λ_{max} = 625 and >1600 nm. The spectra of the parent and end-capped PPE-based anion radicals are identical, which again supports the conclusion that the electron is on the PPE chain, and it is not localized on the T_3 end groups.

Now we turn to consider the spectra of the PAE-based cation radicals. Figure 4c compares the spectra of $T_3^{\bullet+}$, $PBpE_{21}^{\bullet+}$, and $T_3PBpE_{12}^{\bullet+}$. Consistent with the Zindo/S predictions, all of the spectra feature two strong absorption bands, one in the visible and a second in the near-IR. The bands are observed at λ_{max} = 550 and 850 nm in $T_3^{\bullet+}$, in good agreement with the previously reported spectrum of this species.[60] The two bands appear at

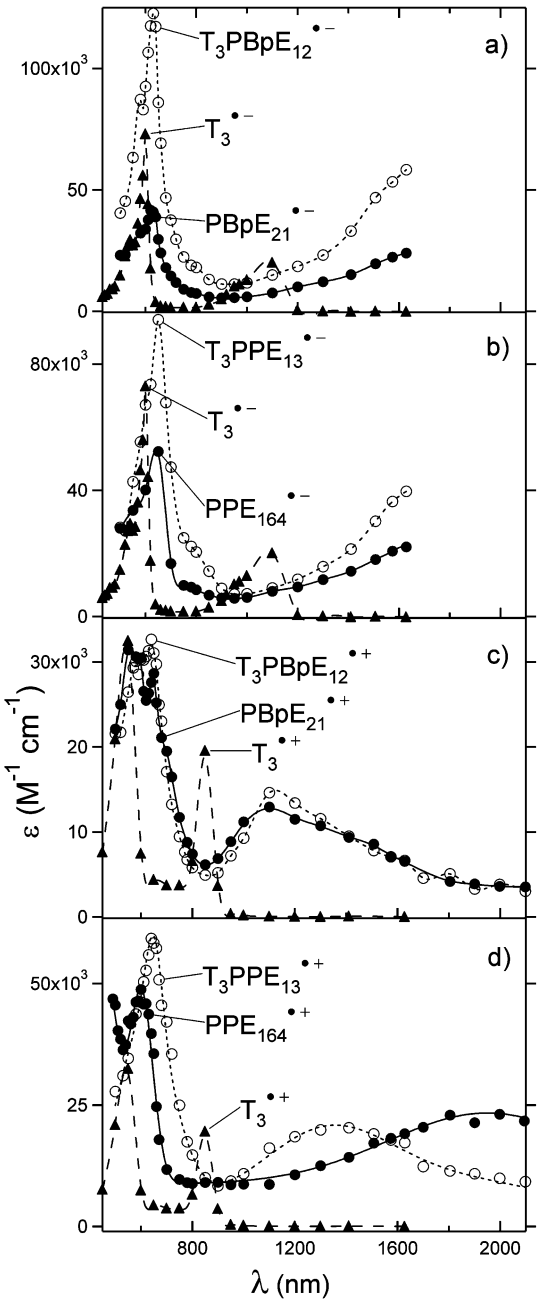

Figure 4. Spectra of cations and anions of poly(arylene ethynylenes) (●), end-capped poly(arylene ethynylenes) (○) and T_3 (▲) where (a) is the spectrum of $PBpE_{21}^{\bullet-}$, $T_3PBpE_{12}^{\bullet-}$ and $T_3^{\bullet-}$ in THF, (b) is the spectrum of $PPE_{164}^{\bullet-}$, $T_3PPE_{13}^{\bullet-}$ and $T_3^{\bullet-}$ in THF, (c) is the spectrum of $PBpE_{21}^{\bullet+}$ and $T_3PBpE_{12}^{\bullet+}$ in DCE/toluene and $T_3^{\bullet+}$ in DCE, and (d) is the spectrum of $PPE_{164}^{\bullet+}$ and $T_3PPE_{13}^{\bullet+}$ in DCE/toluene and $T_3^{\bullet+}$ in DCE. The polymer concentrations were in the range 0.6−2.8 mM in repeat units, and delay times were in the range 0.1−1.0 μs.

λ_{max} = 600 and 1150 nm in $PBpE_{21}^{\bullet+}$ and $T_3PBpE_{12}^{\bullet+}$. The most significant feature with respect to the data for the PBpE-based cation radicals is that the spectra of the parent and T_3 end-capped polymers are essentially identical. This finding strongly suggests that in $T_3PBpE_{12}^{\bullet+}$ the hole resides in the PBpE chain; that is, it is not trapped by and localized on the T_3 end-groups. This result was initially a surprise, but on the basis of oxidation potentials estimated by bimolecular hole transfer equilibrium experiments (see below), it is evident that the E_{ox} value for T_3 is slightly greater than that of PBpE, and therefore, at equilibrium, $PBpE^{\bullet+}$ is favored (i.e., the equilibrium lies to

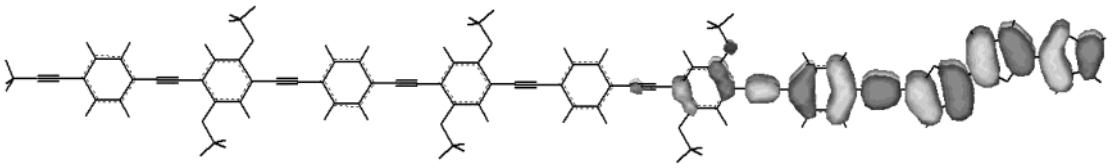

Figure 5. Segment of a PPE-based polymer featuring seven phenylene ethynylene units attached to a terthiophene unit (at right). The HOMO, computed by AM1, is principally on T_3 but also penetrates into the PPE.

the left in eq 6

$$T_3-(PBpE^{\bullet+})-T_3 \rightleftarrows T_3-(PBpE)-T_3^{\bullet+} \qquad (6)$$

Finally, Figure 4d compares the spectra of $PPE_{164}^{\bullet+}$ and $T_3PPE_{13}^{\bullet+}$. It is immediately clear that the spectra of these species are not the same. Specifically, $PPE_{164}^{\bullet+}$ features two bands at $\lambda_{max} = 600$ and 1950 nm, and in $T_3PPE_{13}^{\bullet+}$, the visible band is red-shifted to $\lambda_{max} = 640$ nm and the near-IR band is blue-shifted to $\lambda_{max} = 1350$ nm. The spectrum of $PPE_{24}^{\bullet+}$ (not shown) was the same as that of $PPE_{164}^{\bullet+}$. This result indicates that the difference in the spectra of $PPE_{164}^{\bullet+}$ and $T_3PPE_{13}^{\bullet+}$ is not simply due to the difference in the median chain length of the two polymers. The fact that the cation radical of the T_3 end-capped polymer is different from that of the parent strongly implies that the hole is trapped on the T_3 end-group. However, although it is evident that the presence of the T_3 end-groups has an effect on the spectrum of the cation radical, the spectrum is distinctly different from that of the oligomer cation radical, $T_3^{\bullet+}$. In particular, the low-energy transition in $T_3PPE_{13}^{\bullet+}$ is red-shifted and considerably broader compared to the low energy transition in $T_3^{\bullet+}$. This suggests that the hole is not localized on the T_3 end-cap, but rather it is delocalized into the PPE segment. This notion is supported by the fact that the absorption spectrum of $Ph\text{-}T_3^{+\bullet}$ (see the Supporting Information for spectrum, $\lambda_{max} =$ 625 and 1040 nm) features bands that are at wavelengths that are "in between" those observed for $T_3^{\bullet+}$ and $T_3PPE_{13}^{\bullet+}$. The fact that the absorption bands of $Ph-T_3^{+\bullet}$ are red-shifted relative to those of $T_3^{\bullet+}$ shows that the SOMO in $Ph-T_3^{+\bullet}$ is delocalized into the phenylene ethynylene unit. Moreover, the fact that the absorption bands of $T_3PPE_{13}^{\bullet+}$ are red-shifted relative to those of $Ph-T_3^{+\bullet}$ suggests that in the end-capped polymer the SOMO in the cation radical likely penetrates a few phenylene ethynylene units into the chain.

Additional insight concerning the electronic structure of $T_3PPE_{13}^{\bullet+}$ comes from a MO calculation (AM1) of a model PPE oligomer that is end-capped with T_3. As expected based on the spectroscopic results, the AM1 calculation indicates that, although the HOMO in the neutral oligomer is localized primarily on the T_3 unit, it still has significant density extending a few phenylene rings into the PPE segement (see Figure 5 for a plot). Thus, in $T_3PPE_{13}^{\bullet+}$, the charge density is neither fully delocalized into the PPE chain nor is it *localized* on the T_3 end-group. Instead, it is partly localized on an extended electronic system consisting of one T_3 and a few PPE units. This provides an explanation for the observation that the absorption spectrum of $T_3PPE_{13}^{\bullet+}$ is not a simple linear combination of spectra for $T_3^{\bullet+}$ and $PPE_{164}^{\bullet+}$. Moreover, the fact that the low energy absorption band in $T_3PPE_{13}^{\bullet+}$ is red-shifted and broader than in $T_3^{\bullet+}$ or $Ph-T_3^{+\bullet}$ supports the notion that in the end-capped polymer the hole is significantly more delocalized than in either oligomer. It is also notable that, as suggested by the bimolecular hole-transfer equilibrium studies outlined below, there is likely to be an equilibrium established involving hole-transfer from the T_3 end-group to the PPE main chain, i.e.

$$T_3-(PPE^{\bullet+})-T_3 \rightleftarrows T_3-(PPE)-T_3^{\bullet+} \qquad (7)$$

The existence of this equilibrium may also have an influence on the observed spectrum.

Bimolecular Hole Transfer Reactions: Thermodynamics of Intrachain PPE → T_3 Hole Transfer. To explain the surprising result that the hole is not trapped by the T_3 end-groups in $T_3PBpE_{12}^{\bullet+}$, bimolecular hole-transfer experiments were carried out between the polymers and the series of α-thiophene oligomers (T_n, where $n = 2-4$) to determine the energetics of intrachain hole transfer. These experiments were designed to measure the position of the equilibrium (and the rate constants) for the following series of hole transfer reactions:

$$PAE^{\bullet+} + T_2 \rightleftarrows PAE + T_2^{\bullet+} \qquad (8a)$$

$$PAE^{\bullet+} + T_3 \rightleftarrows PAE + T_3^{\bullet+} \qquad (8b)$$

$$PAE^{\bullet+} + T_4 \rightleftarrows PAE + T_4^{\bullet+} \qquad (8c)$$

By using the reported potentials for the $T_n^{0/\bullet+}$ couples[61] along with the experimentally determined equilibrium constants for hole transfer from each $PAE^{\bullet+}$ to T_3 (i.e., K_{eq} for eq 8b), redox potentials (E°_{ox}) for the polymers were determined.[62] Table 2 compiles the experimentally determined rate and equilibrium constant data, and Figure 6 provides a redox scale summarizing the E°_{ox} values, and an example of the data used in these measurements is provided in the Supporting Information section. These measurements clearly show that the oxidation potentials of all of the polymers are bracketed between the potentials for T_2 and T_4 (i.e., 1.25 V > E°_{ox} > 0.80 V), while equilibria are established with T_3.

The potentials extracted from the bimolecular hole transfer experiments provide an explanation for the observations that T_3 end-cap groups capture holes in T_3PPE_{13}, but not in the biphenyl-based polymer T_3PBpE_{12}. Specifically, E°_{ox} for the PAE chain in the biphenyl-based polymers is 100 mV lower than that of the phenylene polymers. This difference is large enough to cause the hole transfer equilibrium to lie to the left for the biphenylene polymers (as shown in eq 6) and to the right for the phenylene polymers (as shown in eq 7). Another interesting finding of the bimolecular hole transfer equilibria is that injection of a hole into PPE_{164} is thermodynamically favored over injection into PPE_{24} by a factor $K_{eq}(164)/K_{eq}(24) = 8 \pm 2.5$. This factor is close to the ratio of the polymer chain lengths (6.8) and almost certainly reflects entropic factors which favor the hole on the longer PPE chain. If the delocalization length of a charge carrier is L polymer repeat units, the number of ways to place carrier in the polymer of length n is $n - L$; therefore, the ratio of equilibrium constants for two polymers of lengths n_1 and n_2 should be $K(n_1)/K(n_2) = (n_1 - L)/(n_2 - L)$. Consequently, the present results are compatible with a delocalization length, L, of less than 10 polymer repeat units (20 phenylene ethynylene units). Note that K_{eq} for reaction 8b

TABLE 2: Rates and Equilibrium Constants for Hole Transfer from Polymer Radical Cations to Thiophene Oligomers (See Note *a* Regarding Uncertainties)

reaction	*n*	k (M^{-1} s^{-1})	K_{eq}	$\Delta G°$ (*mV*)[a]	E_{ox} (V) vs SCE
$PPE_{164}^{\bullet+} + T_2$	164	$-(2.5 \pm 1.5) \times 10^{11}$ [c]	$(1.0 \pm 0.5) \times 10^{-3}$	177 ± 40	1.03 ± 0.04
$PPE_{164}^{\bullet+} + T_3$	164	4.5×10^9	0.82	5.2	0.91[a]
$PPE_{24}^{\bullet+} + T_3$	24	3.6×10^9	6.0 ± 2	-46	0.96[a]
$PPE_{164}^{\bullet+} + T_4$	164	5.6×10^9	>1.7	< -14	
$PBpE_{21}^{\bullet+} + T_2$	21		$<4.1 \times 10^{-2}$	> 82	<1.13
$PBpE_{21}^{\bullet+} + T_3$	21		0.12	55	0.86[a]
$PBpE_{21}^{\bullet+} + T_4$	21	4.4×10^9	>6.3	< -47	>0.81[a]
$T_3PPE_{13}^{\bullet+} + T_3$	13		1.1	-1.3	0.91[a]
$T_3PPE_{13}^{\bullet+} + T_4$	13	3.8×10^9	>45	< -98	>0.86[a]

[a] Estimated uncertainties in $-\Delta G°$ or E_{ox} are ($+$ 10, $-$40 mV) for reactions with T_3 and T_4 due to uncertain contributions from a second oxidizing species and to formation of an unknown species at longer times (see text). [b] Oxidation potentials for the polymers based on reported potentials $E°_{ox} = 1.25$ (T_2), 0.95 (T_3) and 0.80 (T_4) in V vs Ag/AgCl[61] were converted to SCE reference by subtracting 44 mV to give 1.21, 0.91 and 0.76. See note *a*. [c] The sign indicates that this is the reverse reaction. Only the reverse reaction (a transfer of charge from $T_2^{+\bullet}$ to PPE) was observed.

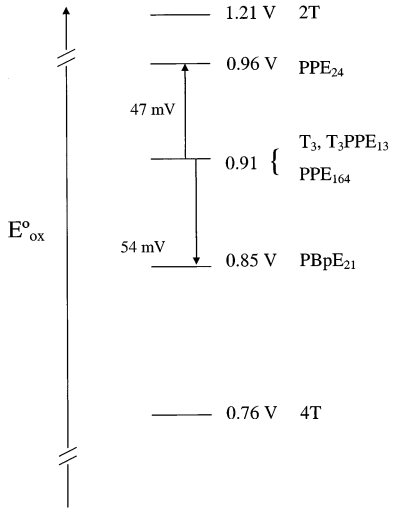

Figure 6. Oxidation potentials vs SCE for polymers investigated, obtained from measured equilibrium constants for bimolecular charge-transfer reactions with terthiophene in DCE/toluene solution (see Table 2).

is ≈1.0 for T_3PPE_{13}, which leads to the surprising conclusion that the cation of the T_3 end-cap is *not* stabilized relative to T_3 by conjugation with PPE and is instead slightly destabilized. This result may reflect a balance between the expected electron withdrawing effect of the PPE-segment[63] on the T_3 unit and the stabilizing effect of delocalization of the T_3 HOMO into the PPE chain.

Typically, the use of electron transfer equilibria to obtain oxidation potentials affords values errors of only a few mV; however, the certainties of the equilibrium constants and free energy changes for the equilibria studied herein are reduced due to complexities. Specifically, the Cl•−toluene π-charge transfer complex (Cl:PhMe) mentioned above appears to oxidize the PAEs slowly (if at all), but it does oxidize T_3 or T_4 to their radical cations. This fact and the limited lifetime of Cl:PhMe lead to a variable number of ions entering the equilibria of reaction 8 that changes with the concentration of T_3 or T_4. The "extra" ions are included in the calculations of K_{eq}'s, but estimation of their amounts contributes to uncertainty. A second complexity that arises is related to the slow formation of an unknown species, possibly a hetero-dimer between T_3 and $PAE^{\bullet+}$ that limits our ability to work at higher reactant concentrations. These effects contribute to the uncertainties reported for the free energy changes in Table 2.

Dynamics of Intrachain Hole Transfer. As noted in the Introduction, a long-term objective of this work is to determine the dynamics of intramolecular hole transfer through a π-conjugated system (k_{HT}, eq 1). When holes are attached to T_3PPE_{13} most (i.e., > 80%) are likely to be initially captured by the long PPE segments, which consist on average of 26 phenylene rings and are over 15 nm in length. The preference for initial hole transfer from the primary donor $(PhMe)_2^{\bullet+}$ to the PPE chain arises because the process is very exothermic ($\Delta G° < -0.5$ eV) and because the chain is present in significant molar excess relative to the T_3 end-groups (ca. 8:1). Nevertheless, the final product, $T_3PPE_{13}^{\bullet+}$, in which the hole is trapped by T_3 end-group, is observed at the earliest accessible time scale in the pulse radiolysis experiments, demonstrating that intramolecular hole transport from the main chain of T_3PPE_{13} to a T_3 end cap occurs faster than the bimolecular capture of holes from the solvent. Due to solubility constraints, the maximum concentration of T_3PPE_{13} used in the hole transfer experiments was 1.6 mM. Under these conditions the growth of the radical cation occurred over ∼40 ns, with a bimolecular attachment rate constant of 3.6×10^{10} M^{-1} s^{-1}.

Assuming that the absorption spectrum of holes in the chain is similar to that observed for $PAE^{\bullet+}$, a lower limit of $k_{HT} \geq 1 \times 10^8$ s^{-1} is placed on the rate of hole transfer from the polymer to the end-caps on the basis of the observed radical cation growth rate. The result, $k_{HT} \geq 1 \times 10^8$ s^{-1}, is similar to the lower limit determined by Matsui et al.[64] for electron transfer from the σ-conjugated silicon backbone of poly(methylphenylsilane) to a tetraphenylporphyrin side chain via a saturated ether linkage. The present experiments show that transport of holes is rapid in a π-conjugated polymer. That result is expected from the optical spectra of the polymers without end caps, which indicate that the charges occupy well-delocalized states. Charge transport is probably much faster than the limit established by the present observations, pointing to the desirability of much faster methods for injecting polarons into the polymers and for the study of end-capped polymers with considerably longer chains.

Summary and Conclusion

A new series of PAEs that are end-capped with α-terthiophene groups have been synthesized and characterized by NMR, GPC, and optical spectroscopy. The T_3 end-capped polymers have moderate molecular weights, and the available information indicates that the end-capping process is efficient. The absorption spectra of the T_3 end-capped polymers and the parent polymers are very similar; however, the fluorescence spectra of the end-capped polymers feature a significantly enhanced intensity on the long-wavelength side of the fluorescence band. The fluorescence results indicate that, although the singlet

excited state wave function resides principally on the T_3 end-groups, it is still somewhat delocalized into the PPE segment. This conclusion is supported by AM1 molecular orbital calculations which show that the HOMO of the T_3 end-capped polymer penetrates into the PPE chain.

Pulse radiolysis was used to produce the anions and cations of the parent and T_3 end-capped polymers. Electron and hole transfer from the solvated electrons and solvent-based holes to the PPE chains follow bimolecular kinetics, with rate constants that are close to diffusion controlled when consideration is made for the length of the rigid-rod polymers. The absorption spectra of the PAE-based cation and anion radicals are similar with two strongly allowed transitions, one in the visible ($\lambda_{max} = 600$ nm) and a second in the near-IR. The spectra are in qualitative agreement with spectra simulated by Zindo/S calculations. The calculations also provide insight into the electronic structure of the cation radicals in the T_3 end-capped polymers. Specifically, they suggest that in T_3 end-capped PPE polymer the hole resides in an orbital that is largely located on the T_3 chain end, but it still penetrates significantly into the PPE chain. The experimental spectra on the cation radicals of the T_3 end-capped polymers reveal that the holes are localized on (or trapped by) the T_3 end-groups in the phenylene polymers but not in the biphenylene polymers. Bimolecular hole transfer studies explain this surprising result by showing that the PAE chain has an E°_{ox} value that is ≈100 mV less than that of the T_3 end-group.

Kinetics measurements carried out on T_3PPE_{13} indicate that intrachain hole transfer occurs much faster than bimolecular hole capture by the polymer, indicating that k_{HT} is greater than 1×10^8 s^{-1}. Experiments in progress seek to observe intrachain electron transfer in PPE-based polymers that contain electron trap end-groups. The results of this work will be reported soon.

Acknowledgment. Work at Brookhaven National Laboratory was supported by the U.S. Department of Energy, Division of Chemical Sciences, Office of Basic Energy Sciences, under Contract DE-AC02-98-CH10886. Work at the University of Florida was supported by the National Science Foundation (Grant No. CHE-0211252).

Supporting Information Available: Synthesis of starting materials, table of photophysical data, example data from bimolecular hole transfer experiments, the difference absorption spectrum of Ph-$T_3^{+\bullet}$, and a labeled ^1H NMR spectrum of T_3-PPE_{13} (8 pages). This material is available free of charge via the Internet at http://pubs.acs.org.

References and Notes

(1) Skotheim, T. A., Elsenbaumer, R. L., Reynolds, J. R., Eds.; *Handbook of Conducting Polymers*, 2nd ed.; Marcel Dekker: New York, 1998.

(2) McGehee, M. D.; Miller, E. K.; Moses, D.; Heeger, A. J. In *Advances in Synthetic Metals. Twenty Years of Progress in Science and Technology*; Bernier, P., Lefrant, S., Bidan, G., Eds.; Elsevier: Amsterdam, 1999; pp 98−205.

(3) Babel, A.; Jenekhe, S. A. *J. Phys. Chem. B* **2003**, *107*, 1749−1754.

(4) Kokil, A.; Shiyanovskaya, I.; Singer, K. D.; Weder, C. *J. Am. Chem. Soc.* **2002**, *124*, 9978−9979.

(5) Campbell, I. H.; Smith, D. L.; Neef, C. J.; Ferraris, J. P. *App. Phys. Lett.* **1999**, *74*, 2809−2811.

(6) Sirringhaus, H.; Tessler, N.; Friend, R. H. *Science* **1998**, *280*, 1741−1744.

(7) Fuchigami, H.; Tsumura, A.; Koezuka, H. *App. Phys. Lett.* **1993**, *63*, 1372−1374.

(8) Harrison, B. S.; Ramey, M. B.; Reynolds, J. R.; Schanze, K. S. *J. Am. Chem. Soc.* **2000**, *122*, 8561−8562.

(9) Tan, C.; Pinto, M. R.; Schanze, K. S. *Chem. Commun.* **2002**, 446−447.

(10) Liu, Y.; Jiang, S.; Schanze, K. S. *Chem. Commun.* **2003**, 650−651.

(11) Bumm, L. A.; Arnold, J. J.; Cygan, M. T.; Dunbar, T. D.; Burgin, T. P.; Jones, L.; Allara, D. L.; Tour, J. M.; Weiss, P. S. *Science* **1996**, *271*, 1705−1707.

(12) Adams, D.; Brus, L.; Chidsey, C. E. D.; Creager, S.; Creutz, C.; Kagan, C. R.; Kamat, P.; Lieberman, M.; Lindsay, S.; Marcus, R. A.; Metzger, R. M.; Michel-Beyerle, M. E.; Miller, J. R.; Newton, M. D.; Rolison, D. R.; Sankey, O.; Schanze, K. S.; Yardley, J.; Zhu, X. *J. Phys. Chem. B* **2003**, *107*, 6668−6697.

(13) Candeias, L. P.; Grozema, F. C.; Padmanaban, G.; Ramakrishnan, S.; Siebbeles, L. D. A.; Warman, J. M. *J. Phys. Chem. B* **2003**, *107*, 1554−1558.

(14) Zhou, Q.; Swager, T. M. *J. Am. Chem. Soc.* **1995**, *117*, 12593−12602.

(15) Swager, T. M. *Acc. Chem. Res.* **1998**, *31*, 201−207.

(16) Chen, L. X.; Jäger, W. J. H.; Niemczyk, M. P.; Wasielewski, M. R. *J. Phys. Chem. A* **1999**, *103*, 4341−4351.

(17) Wang, B.; Wasielewski, M. R. *J. Am. Chem. Soc.* **1997**, *119*, 12−21.

(18) Zhang, Y.; Murphy, C. B.; Jones, W. E. *Macromolecules* **2002**, *35*, 630−636.

(19) Chen, L.; McBranch, D. W.; Wang, H.-L.; Helgeson, R.; Wudl, F.; Whitten, D. G. *Proc. Natl. Acad. Sci. U.S.A.* **1999**, *96*, 12287−12292.

(20) Tan, C.; Pinto, M. R.; Schanze, K. S. *Chem. Commun.* **2002**, 446−447.

(21) Wang, J.; Wang, D. L.; Miller, E. K.; Moses, D.; Bazan, G. C.; Heeger, A. J. *Macromolecules* **2000**, *33*, 5153−5158.

(22) Swager, T. M.; Gil, C. J.; Wrighton, M. S. *J. Phys. Chem.* **1995**, *99*, 4886−4893.

(23) Pschirer, N. G.; Byrd, K.; Bunz, U. H. F. *Macromolecules* **2001**, *34*, 8590−8592.

(24) Beljonne, D.; Pourtois, G.; Silva, C.; Hennebicq, E.; Herz, L. M.; Friend, R. H.; Scholes, G. D.; Setayesh, S.; Mullen, K.; Bredas, J. L. *Proc. Natl. Acad. Sci. U.S.A.* **2002**, *99*, 10982−10987.

(25) Bunz, U. H. F. *Chem. Rev.* **2000**, *100*, 1605−1644.

(26) Wishart, J. F. In *Radiation Chemistry: Present Status and Future Trends*; Jonah, C. D., Rao, B. S. M., Eds.; Elsevier Science: Amsterdam, 2001; Vol. 87, pp 21−35.

(27) Boas, U.; Dhanabalan, A.; Greve, D. R.; Meijer, E. W. *Synlett* **2001**, 634−636.

(28) Murov, S. L.; Carmichael, I.; Hug, G. L. *Handbook of Photochemistry*, 2nd ed.; Marcel Dekker: New York, 1993.

(29) Demas, J. N.; Crosby, G. A. *J. Phys. Chem.* **1971**, *75*, 991−1024.

(30) Wishart, J. F.; Cook, A. R. *Rev. Sci. Inst.* **2003**, To be submitted.

(31) Wang, Y.; Tria, J. J.; Dorfman, L. M. *J. Phys. Chem.* **1979**, *83*, 1944−1951.

(32) Beaumond, D.; Rodgers, M. A. J. *Trans. Faraday. Soc.* **1969**, *65*, 2973−2980.

(33) Matsui, M.; Imamura, M.; Karasawa, T. *IPCR Cyclotron Prog. Rep.* **1970**, *4*, 126−127.

(34) Bockrath, B.; Dorfman, L. M. *J. Phys. Chem.* **1973**, *77*, 2618−2622.

(35) Shaede, E. A.; Kurihara, H.; Dorfman, L. M. *Int. J. Radiat. Phys. Chem.* **1974**, *6*, 47−54.

(36) Dodelet, J.-P.; Freeman, G. R. *Can. J. Chem.* **1975**, *53*, 1263−1274.

(37) Bunz, U. H. F. *Chem. Rev.* **2000**, *100*, 1605−1644.

(38) We estimate that the degree of polymerization values determined by NMR integration have an error of ±10%.

(39) Liu, J. S.; Loewe, R. S.; McCullough, R. D. *Macromolecules* **1999**, *32*, 5777−5785.

(40) Huang, S. L.; Tour, J. M. *J. Am. Chem. Soc.* **1999**, *121*, 4908−4909.

(41) Schumm, J. S.; Pearson, D. L.; Tour, J. M. *Angew. Chem., Int. Ed. Engl.* **1994**, *33*, 1360−1363.

(42) Ricks, H. L.; Choudry, U. H.; Marshall, A. R.; Bunz, U. H. F. *Macromolecules* **2003**, *36*, 1424−1425.

(43) Sluch, M. I.; Godt, A.; Bunz, U. H. F.; Berg, M. A. *J. Am. Chem. Soc.* **2001**, *123*, 6447−6448.

(44) Walters, K. A.; Ley, K. D.; Schanze, K. S. *Chem. Commun.* **1998**, 1115−1116.

(45) Emmi, S. S.; D'Angelantonio, M.; Beggiato, G.; Poggi, G.; Geri, A.; Pietropaolo, D.; Zotti, G. *Radiat. Phys. Chem.* **1999**, *54*, 263−270.

(46) Badger, B.; Brocklehurst, B. *J. Chem. Soc., Faraday Trans.* **1969**, *65*, 2582−2587.

(47) Ohashi, K.; Nakane, Y.; Inokuchi, Y.; Nakai, Y.; Nishi, N. *Chem. Phys.* **1998**, *239*, 429−436.

(48) Funston, A. M.; Miller, J. R. *Radiat. Phys. Chem*. Submitted.

(49) Traytak, S. D. *Chem. Phys. Lett.* **1992**, *197*, 247−254.

(50) Traytak, S. D. *Chem. Phys. Lett.* **1994**, *227*, 180−186.

(51) Grozema, F. C.; Hoofman, R. J. O. M.; Candeias, L. P.; de Haas, M. P.; Warman, J. M.; Siebbeles, L. D. A. *J. Phys. Chem. A* **2003**, *107*, 5976−5986.

(52) Smoluchowski, M. *Zeit. Phys.* **1916**, *17*, 557−571.

(53) Baxendale, J. H.; Beaumond, D.; Rodgers, M. A. J. *Trans. Faraday. Soc.* **1970**, *66*, 1996−2003.

(54) Bockrath, B.; Gavlas, J. F.; Dorfman, L. M. *J. Phys. Chem.* **1975**, *79*, 3064.

(55) Kadhum, A. A. H.; Salmon, G. A. *J. Chem. Soc., Faraday Trans. 1* **1986**, *82*, 2521−2530.

(56) Salmon, G. A.; Seddon, W. A.; Fletcher, J. W. *Can. J. Chem.* **1974**, *52*, 3259−3268.

(57) Halkyard, C. E.; Rampey, M. E.; Kloppenburg, L.; Studer-Martinez, S. L.; Bunz, U. H. F. *Macromolecules* **1998**, *31*, 8655−8659.

(58) Shida, T. *Electronic Absorption Spectra of Radical Ions*; Elsevier Science Publishers B. V.: Amsterdam, 1988.

(59) As a point of reference, the calculations predict that the diphenylacetylene cation radical ($n = 1$) will exhibit two allowed transitions at $\lambda_{max} = 640$ and 406 nm. The computed absorption band maxima compare reasonably well with those determined experimentally ($\lambda_{max} = 805$ and 425 nm, ref 58).

(60) Wintgens, V.; Valat, P.; Garnier, F. *J. Phys. Chem.* **1994**, *98*, 228−232.

(61) Meerholz, K.; Heinze, J. *Electrochim. Acta* **1996**, *41*, 1839−1854.

(62) Attempts to directly measure the oxidation potentials for the PAEs by using electrochemical methods were unsuccessful. Broad, irreversible anodic waves were observed in the range 1.1−1.3 V (vs SCE) for solutions and thin films of the PAEs.

(63) Wang, Y.; Liu, S.; Pinto, M. R.; Dattelbaum, D. M.; Schoonover, J. R.; Schanze, K. S. *J. Phys. Chem. A* **2001**, *105*, 11118−11127.

(64) Matsui, Y.; Nishida, K.; Seki, S.; Yoshida, Y.; Tagawa, S.; Yamada, K.; Imahori, H.; Sakata, Y. *Organometallics* **2002**, *21*, 5144−5147.